Preprint Cambridge Centre for Computational Chemical Engineering ISSN 1473 – 4273

A fully coupled simulation of PAH and soot growths with a population balance model

Dongping Chen, Zakwan Zainuddin, Jethro Akroyd, Sebastian Mosbach, and Markus Kraft [1]

released: 12 January 2012

[1] Department of Chemical Engineering
and Biotechnology
University of Cambridge
New Museums Site
Pembroke Street
Cambridge, CB2 3RA
United Kingdom
E-mail: mk306@cam.ac.uk

Preprint No. 113

Keywords: Soot, Model, Flame, PAH

Edited by
Computational Modelling Group
Department of Chemical Engineering and Biotechnology
University of Cambridge
New Museums Site
Pembroke Street
Cambridge CB2 3RA
United Kingdom

Fax: + 44 (0)1223 334796
E-Mail: c4e@cam.ac.uk
World Wide Web: http://como.cheng.cam.ac.uk/

Abstract

In this paper we present a detailed soot population balance model. In the model, soot nanoparticles are described by primary particles which are made up of individual PAH molecules. This model improves on the previous PAH-PP model (Sander *et al.*, 2011, *Proceedings of the Combustion Institute.* **33** 675–683) as it accounts for particle rounding due to sintering and surface growth, and it fully couples the evolution of PAH and soot particles. For the first time, the model is described in detail and is used to simulate a variety of flames. From the detailed numerical solution, mass spectra and particle size distributions (PSDs) are extracted and compared with experiments. By using a new counting method and a simple collision efficiency model, experimental mass spectra has been qualitatively reproduced and the results fit well with the experimental PSDs of the various flames.

Contents

1 Introduction

Soot is formed from the incomplete combustion of hydrocarbon fuels. It is usually an unwanted byproduct and its formation has attracted a lot of interest from the scientific community. In fact, these nano-sized particles [19] are considered to be one of the most serious pollutants [14]. The smallest observed soot particles are about 1.6 nm in diameter [19]. At this size, these particles can penetrate deep into the human lung and cause severe diseases like cancer and asthma [1]. However, the potential threat of soot is not only limited to human health, but also to the environment. It is responsible for global warming [14] and reduced atmospheric visibility [6]. Therefore, understanding its formation is key to mitigating these problems. The study of soot formation also has the benefit of improving the understanding of formation of other nanoparticles such as silica and titanium dioxide in flame processes [16].

Much experimental and theoretical work has been carried out to investigate soot growth under flame conditions. However, due to the transient and high-temperature nature of combustion, the residence time of intermediate species involved in soot formation is very short; typically milliseconds. It is difficult for experimentalists to obtain data describing the intermediate processes; hence, numerical studies with a detailed model are used. To determine soot characteristics such as PAH inception size and soot density [11, 17], a model describing particles by their mass and surface area is not sufficient and a detailed particle representation is required.

In the previous PAH-PP model [13], soot particles are described by primary particles which are made up of individual PAH molecules. However, only the number of carbon and hydrogen atoms in each PAH molecule are tracked and not the exact PAH structure; therefore, the evolution of PAH and soot particles could not be calculated simultaneously. The underlying reason for this problem is that the detailed representation of the PAH structure has not been fully coupled with the soot structure. Therefore, the purpose of this paper is to present a fully coupled model in detail and to reproduce the mass spectra and PSDs of a number of laminar premixed flames.

2 Model development

2.1 Particle model

To accurately model soot formation, a gas-phase solver and a particle-phase solver are required at the very least. In this work, an external gas-phase chemistry solver (PREMIX package) [7] is used to precalculate the gas-phase species profile up to pyrene and the pyrene formation rate according to the ABF mechanism. The species profile is post-processed by the PAH-PP model to obtain information relating to soot formation. The model is built by coupling the Kinetic Monte Carlo - Aromatic Site (KMC-ARS) model [10] with the previous PAH-PP model [13]. The kinetic Monte Carlo method (KMC) is used to solve population balance equations which describe the evolution of the number density of particles undergoing various transformations. Four types of transfor-

mations have been included in this particle model: inception, heterogenous processes, particle-particle process and particle rounding. The particle model is also capable of predicting simulated mass spectra and particle size distributions which can be useful towards improving our understanding of soot formation. A work flow of the soot model is shown in Figure 1. The parameters listed in Figure 1 will be introduced in Section 2.2.

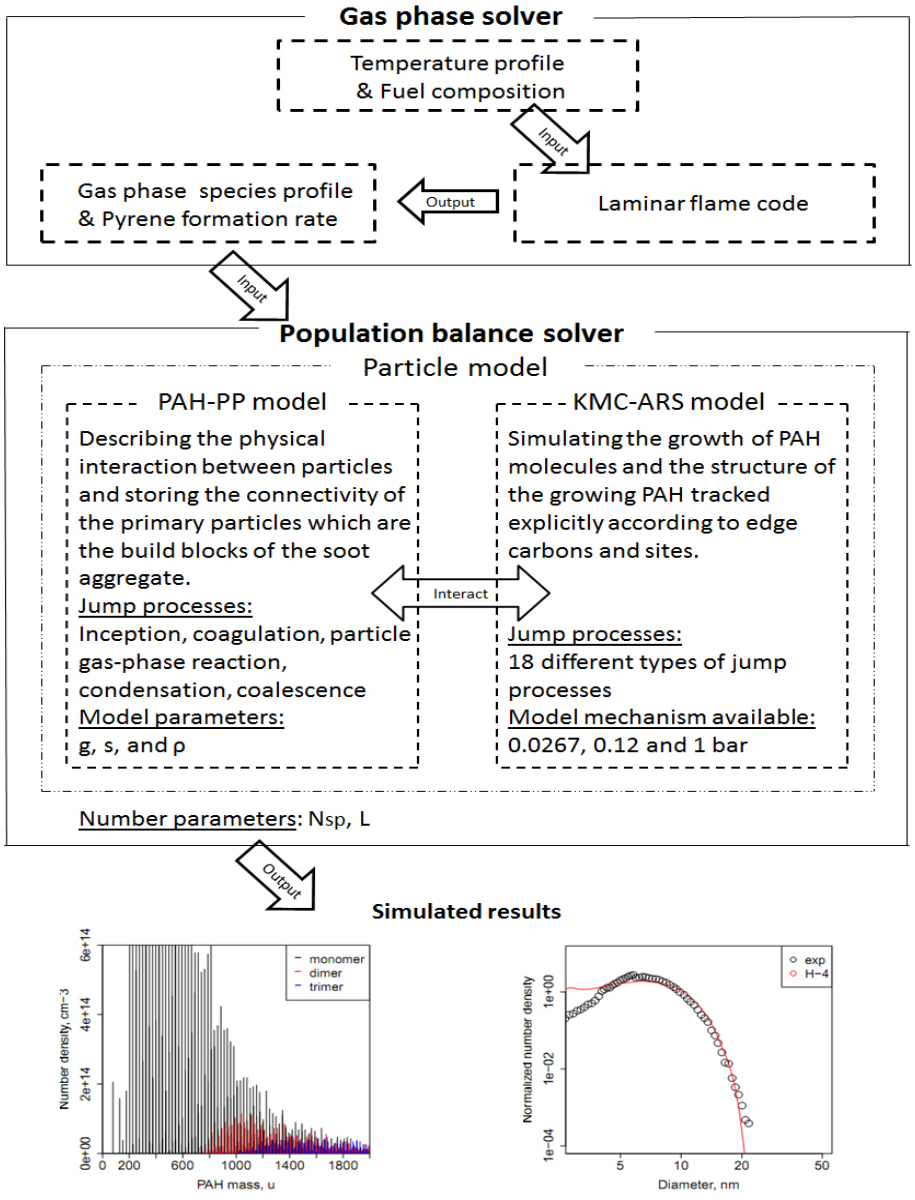

Figure 1: *Work flow of the soot model.*

2.1.1 Type space

A soot particle can be represented as:

$$P_q = P_q(p_1, \ldots, p_n, \mathbf{C}) \tag{1}$$

Particle P_q consists of n primary particles p_i where $i \in \{1, \ldots, n\}$. The state of the system is given by an ensemble of N particles of type P_q where $q \in \{1, \ldots, N\}$. The matrix $\mathbf{C}$ stores the connectivity of various primary particle p_i within soot particle P_q and is described in detail below.

The primary particles can be represented as:

$$p_i = p_i(PAH_1, PAH_2, ..., PAH_j) \tag{2}$$

where PAH_x is the x^{th} species in primary particle p_i and $x \in \{1, \ldots, j\}$.

The matrix $\mathbf{C}$ has dimensions $n \times n$ where n is the number of primary particles in particle P_q and is represented as:

$$\mathbf{C}(P_q) = \begin{pmatrix} 0 & \cdots & 0 & \cdots & 0 \\ \vec{C}_{21} & \ddots & 0 & \cdots & 0 \\ \vdots & \ddots & \ddots & \cdots & \vdots \\ \vec{C}_{i1} & \cdots & \vec{C}_{ij} & \ddots & \vdots \end{pmatrix} \tag{3}$$

The entries $\overrightarrow{C}_{ij}$ of matrix $\mathbf{C}$ are vectors and have the following properties:

$$\vec{C}_{ij} = \begin{cases} 0, \text{ if } p_i \text{ and } p_j \text{ are non-neighbouring}, \\ \text{Common surface area of primary particles } p_i \text{ and } p_j, \\ \text{if they are neighbouring.} \end{cases} \tag{4}$$

These vectors store the common surface area between neighbouring primary particles that changes due to surface growth and condensation, and is used to calculate the rounding between neighbouring primary particles.

The PAH-PP model fully describes the structures of PAHs within primary particles and it allows the evolution of PAHs and soot particles to be simulated simultaneously; thus, the positions of the C atoms and sites in individual PAHs are required and recorded. Here, a PAH planar structure is assumed as in the KMC-ARS model [10]. Since the structure of a planar molecule can be visualised just by knowing the structure at the edges, it is not necessary to track the bulk C atoms. Thus the simplest type space required to track the structure of a PAH only includes the positions of the edge C atoms and their connectivity. Furthermore, this simplified implementation is compartmentally less expensive.

The type space of PAH_j is represented by internal variables η_{C} and η_{S} as:

$$PAH_j = PAH_j(\eta_{\text{C}}, \eta_{\text{S}}) \tag{5}$$

where η_C and η_S are edge carbons and site types respectively in a particular PAH molecule. Figure 2 presents a PAH molecule with different types of sites: free-edges (FE), zigzags (ZZ), armchairs (AC), bays (BY) and five-member rings (R5).

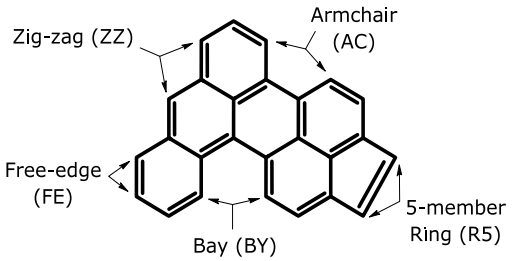

Figure 2: *PAH molecule showing the principal types of surface site [11].*

2.1.2 Particle transformation

In this model, four different types of particle transformations are included and are responsible for soot mass and size growth:

Inception: A particle is formed by the sticking of two individual PAHs. The rate of particle inception is dependent on the collision efficiency [11], the transition regime coagulation kernel [8] and the concentrations of these two PAHs. The particle inception event is described by:

$$\begin{aligned} P_i(p_1(PAH_1), \mathbf{C}(P_i)) + P_j(p_1(PAH_2), \mathbf{C}(P_j)) \rightarrow \\ P_k(p_1(PAH_1, PAH_2), \mathbf{C}(P_k)). \end{aligned} \tag{6}$$

The growth rate of PAHs within particles is slower due to limited accessibility and blocked sites. A model parameter (growth factor) is used to adjust this rate accordingly [13].

Particle-particle process: In this model, coagulation is considered to be the only particle-particle process. In such an event, two particles P_i and P_j collide and stick together with only point contact forming a larger particle which contains the primary particles of the two colliding particles:

$$\begin{aligned} P_i(p_1, ..., p_m, \mathbf{C}(P_i)) + P_j(p_1^*, ..., p_n^*, \mathbf{C}(P_j)) \rightarrow \\ P_k(p_1, ..., p_m, p_1^*, ..., p_n^*, \mathbf{C}(P_k)). \end{aligned} \tag{7}$$

The superscript $*$ indicates primary particles in different soot particles.

Heterogeneous processes: The current particle model considers a heterogeneous processes to be either condensation or a particle gas-phase reaction. Condensation is implemented by adding a PAH_{j+1} from the gas-phase to a primary particle p_k within the particle P_k:

$$\begin{aligned} p_k(PAH_1, ..., PAH_j, \mathbf{C}(P_k)) \rightarrow \\ p_k(PAH_1, ..., PAH_j, PAH_{j+1}, \mathbf{C}(P_k^*)). \end{aligned} \tag{8}$$

A particle gas-phase reaction event is a reaction between a species s_{gas} from the gas-phase and a PAH_l within the primary particle p_k. The product of the reaction

is $PAH_l^* = PAH_l \oplus s_{gas}$ and the implementation of this event is:

$$\begin{aligned} p_k(PAH_1, ..., PAH_l, PAH_j, \mathbf{C}(P_k)) + s_{gas} \rightarrow \\ p_k(PAH_1, ..., PAH_l^*, ..., PAH_j, \mathbf{C}(P_k^*)). \end{aligned} \tag{9}$$

During heterogeneous processes, the matrix $\mathbf{C}(P_k)$ of particle P_i should be updated to $\mathbf{C}(P_k^*)$ to record the change in sphericity of the particles which is discussed below.

Particle rounding: Two processes lead to particle rounding: mass addition and rearrangement of molecules in two adjacent primary particles which is similar to sintering in inorganic nanoparticles. To describe the change in the particle sphericity, a rounding level $R(p_i, p_j)$ is defined as:

$$R(p_i, p_j) = \frac{\frac{S_{\text{sph}}(p_i, p_j)}{C_{ij}} - 2^{-\frac{1}{3}}}{1 - 2^{-\frac{1}{3}}} \tag{10}$$

where $S_{\text{sph}}(p_i, p_j)$ and C_{ij} are the spherical surface area and the common surface area, respectively, of the two neighbouring primary particles p_i and p_j. It is worth noting that the particle is initially assumed to be spherical. The change in the common surface area ΔC_{ij} between the two primary particles p_i and p_j can be calculated [9] as:

$$\Delta C_{ij} = \Delta V_{ij} \frac{s}{r_{ij}^{\text{sph}}} \tag{11}$$

where ΔV_{ij} is the increase in volume of the primary particles p_i and p_j due to condensation or surface reactions, and r_{ij}^{sph} is the radius of a sphere with the equivalent volume of the two particles. The smoothing factor s determines how fast the two primary particles coalesce [9].

Once $R(p_i, p_j)$ exceeds 0.99 the two individual primary particles p_i and p_j are instantly replaced by one primary particle p_l^* containing the species of the previous two particles. Particle rounding is implemented as follows:

$$P_k(p_1, ..., p_i, ..., p_j, ..., p_n, \mathbf{C}(P_k)) \rightarrow P_k^*(p_1, ..., p_l^*, ..., p_{n-1}, \mathbf{C}(P_k^*)). \tag{12}$$

The matrix $\mathbf{C}$, which stores the common surface area of neighbouring primary particles, must be updated after these four different particle transformations. Details on how to update it can be found elsewhere [12]. Besides these transformations, fragmentation of soot particles has been found to significantly affect the PSDs [2]. However, none of the current numerical models have included this transformation. In future, it will be implemented in the PAH-PP model.

2.2 Model parameters

In Sander's recent work [13], the three model parameters were estimated using low discrepancy sequence optimisation and response surface optimisation through fitting to the

Table 1: *Summary of the input parameters to the particle model*

Name	Variable	Value
	Model parameters	
Soot density	ρ	$1.47\ \mathrm{g/cm^3}$
Smoothing factor	s	0.98
Growth factor	g	0.05
	Numerical parameters	
Number of stochastic particles	N_{sp}	16384
Number of repetition	L	5

median of the experimental PSDs, and the results showed excellent agreement with experiments. Therefore, all the simulations in this paper used the same parameters (Table 1). The accuracy of the simulated results is dependent on several numerical parameters to the particle solver. 16384 stochastic particles and 5 repetitions (Table 1) are used to produce simulated results with limited statistical errors according to a convergence analysis. Further increasing these values do not significantly affect the results.

3 Simulation results

3.1 Simulated flames

Table 2 lists the initial conditions of the laminar premixed flames used in this paper. Flames 1-5 are low-pressure flames and are obtained through laser ionisation mass spectrometry (LIMS). These flames are chosen because of the availability of experimentally observed mass spectra of PAH clusters - monomers and dimers [3]. Flames A2, A3 and B3 are atmospheric-pressure flames and are obtained through online sampling and the use of a scanning mobility particle sizer (SMPS) [21]. Through this technique, the size distribution of particles as small as 2.5 nm is measured rapidly and simultaneously which allows a quantitative comparison with computed results.

Table 2: *Laminar premixed flames initial conditions.*

Flame	Fuel in mole factions			ϕ	Pressure	Inflow velocity	Ref.
	C_2H_4	O_2	Ar		(bar)	(cm s^{-1})	
1	0.5	0.5		3.0	0.08	54.0	[3]
2	0.5	0.5		3.0	0.12	54.0	[3]
3	0.5	0.5		3.0	0.15	54.0	[3]
4	0.5	0.5		3.0	0.18	54.0	[3]
5	0.5	0.5		3.0	0.22	54.0	[3]
A2	0.242	0.379	0.379	1.92	1.0	7.85	[21]
A3	0.242	0.379	0.379	1.92	1.0	10.0	[21]
B3	0.242	0.379	0.379	1.92	1.0	8.0	[21]

3.2 Simulated study against low-pressure flames

In the PAH-PP model, the collision of two PAHs does not always create a soot particle; thus, a probability of successful collision (collision efficiency, CE) is introduced. To understand the soot inception process, simple step functions is proposed in this paper to reproduce the mass spectra and PSDs. Specifically, the number of carbons in a particular PAH molecule is compared with a predefined threshold; if exceeded, the sticking of colliding PAHs is always successful, otherwise the sticking fails. A more complex form of the CE model in [11] has not been used in this paper to simplify the analysis. In this work, four different modes (min, max, combined and reduced)have been implemented. In the min and max modes, the collision efficiency of colliding particles is dependent on the smaller and larger mass respectively, while the combined and reduced modes are based on the combined mass and reduced mass of two colliding particles.

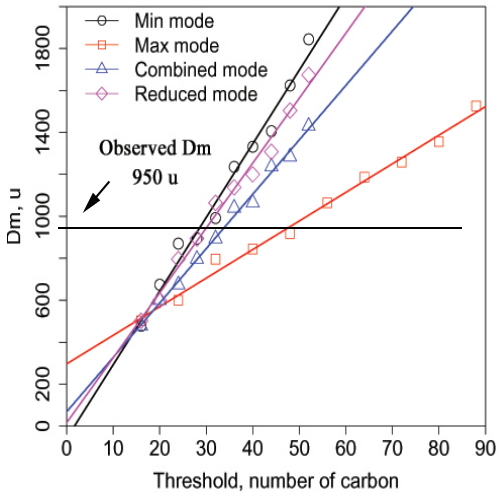

Figure 3: *Summary of D_m for four modes, and indicating that D_m varied with different modes and thresholds. A guideline of observed D_m has been plotted for eye comparison.*

Figure 3 shows that the location of the maxima of the dimer peaks (D_m) is sensitive to the choice of threshold and it is clear that increasing the threshold for a particular mode shifts the D_m to larger PAHs. To reproduce the mass spectra, several CE models (mode of step function - threshold) are selected based on the observed D_m: min-32, max-48, combined-36, and reduced-32. However, the PAH dimer peaks are underestimated (Figure 5a)and to improve on this result a new counting method is applied.

In the low-pressure flames [4, 5], an online laser ionisation mass spectrometry was applied to obtain and analyse the mass spectra of a particular flame. However, using a direct ionising beam instead of a desorption-adsorption sample process may lead to undesired fragmentation of soot particles [18]. Therefore, a new counting method of x-mer is established which assumes that soot particles undergoes strong fragmentation and all primary

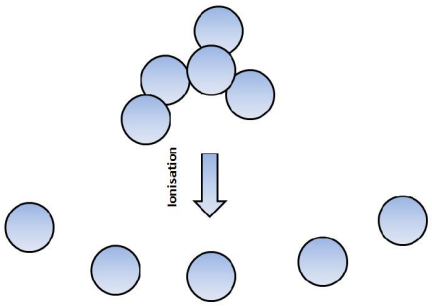

Figure 4: *New counting method assuming primary particles in soot particles separated by ionisation*

particles break apart from each other (Figure 4). Based on this assumption, the dimers and trimers in soot particles composed of various primary particles are counted unlike the ordinary method which only counted soot particles with one primary particle. By using the new method, the predicted amount of dimers and trimers increases significantly (Figure 5b) and there is an overall agreement. Furthermore, a clear monomer decay at approximately 800 u is predicted which is consistent with the experimental observation. In addition, it is important to mention that the predicted D_m is still kept in the range of 992 and 1040 u for the ordinary and new method respectively.

By establishing a simple CE model and a new counting method, the experimental mass spectra are successfully reproduced. This is achieved by assuming that PAHs as small as ovalene ($C_{32}H_{14}$) can stick under flame conditions which is inconsistent with the work of others. According to Raj [11] and Totton [15], the dimerisation of PAH molecules as large as circumcoronene ($C_{54}H_{18}$), at high temperatures, does not produce enough PAH clusters to be significant. This conflict raises the questions of whether ovalene dimers can survive at high temperatures and whether they are responsible for soot inception. There could be other factors which play an important role in soot inception which can decrease the critical soot inception size. In Wang's recent work [18], aromatic π radicals can significantly enhance the binding ability between PAH clusters. He hypothesised that a π-radical-bearing PAH as small as perylene ($C_{20}H_{12}$) can dimerise with other PAH molecules thus forming stacked structures. Depending on how the experiments are interpreted, the choice of counting method is important as it leads to a dramatic variation in the predicted dimer and trimer peaks. In conclusion, the PAH-PP model is a tool to understand the underlying principles and test various hypotheses in the study of soot formation, but this requires further investigation.

3.3 Simulated study against atmospheric-pressure flames

In this section quantitative comparisons are made between the simulated PSDs and the experimental PSDs for atmospheric-pressure flames at various HABs. When making these comparisons, the effects of probe perturbation during the sampling process are important. These effects arise primarily from flame cooling by the probe which affects the gas velocity and the particle growth evolution [20]. To account for these effects, a constant shift of

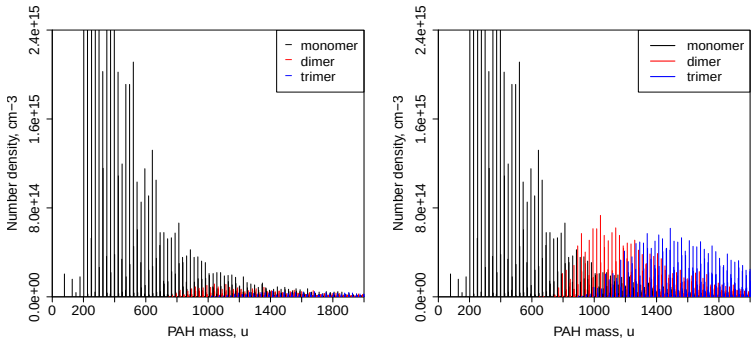

(a) *Simulated mass spectra with old counting method*

(b) *Simulated mass spectra with new counting method*

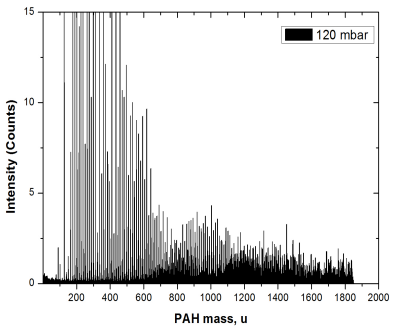

(c) *Experimental mass spectra*

Figure 5: *Simulated results with old and new counting methods for flame 2, using min-32 as CE model, and also an experimental mass spectrum.*

2.5 mm is applied to all the flames. From Figure 6, the simulated PSDs match the shapes of the experiments for all the three cases. According to a brief study, the PSD is insensitive to the critical soot inception size. The overestimation of small particles is also observed in Sander's work [13]. The amount and size of small particles is mainly determined by the gas-phase chemistry which is outside of the scope of this paper. In addition, the three estimated parameters in the previous work may not be valid due to changes in the underlying data structure but the results are surprisingly good. However, the underpredicted PSDs for A2 at high HABs 10 and 12 mm are apparent (Figure 6). Reasons for these are not clear and further investigations are necessary to understand these discrepancies.

4 Conclusions

A detailed soot population balance model, PAH-PP model, is presented in detail. This model is developed by coupling the previous PAH-PP model with the KMC-ARS model. After full coupling, the PAH-PP model is capable of storing the exact structure of PAH molecules within primary particles, and the connectivity between these particles. There-

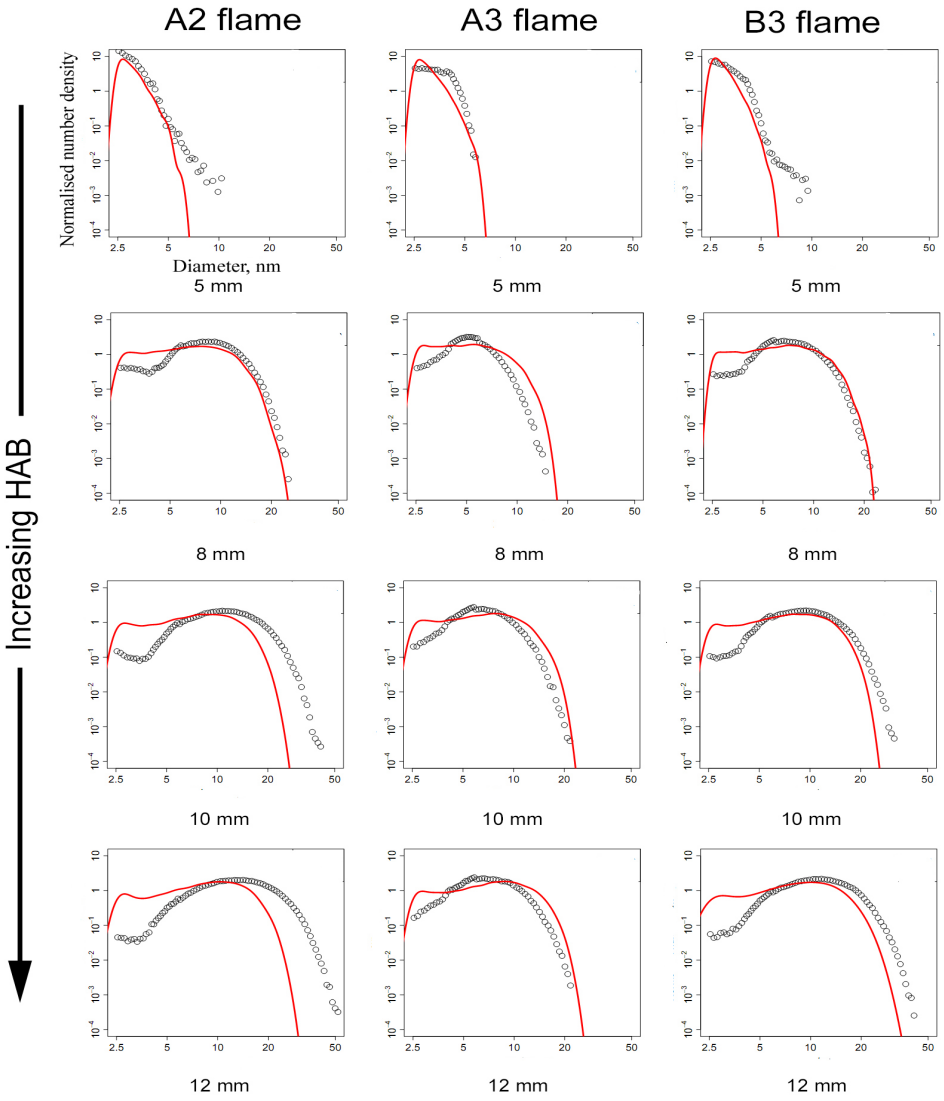

Figure 6: *Simulated and experimental PSDs for the flames A2, A3 and B3 at 5, 8, 10 and 12 mm above the burner. The min-32 CE model is used in the above simulations.*

fore, the evolution of PAH and soot particles can be calculated simultaneously.

With the use of the PAH-PP model, it is the first time the mass spectra and PSDs are generated simultaneously with the same parameter data set. These results show good agreement with experimental observations for a variety of flames. However, the critical soot inception size and counting method has been found to cause large variations in the simulated mass spectra. Although there are still many aspects behind this phenomenon to be investigated, the PAH-PP model can be a useful tool for the study of soot formation.

References

[1] T. R. Barfknecht. Toxicology of soot. *Progress in Energy and Combustion Science*, 9:199–237, 1983.

[2] C. A. Echavarria, I. C. Jaramillo, A. F. Sarofim, and J. S. Lighty. Studies of soot oxidation and fragmentation in a two-stage burner under fuel-lean and fuel-rich conditions. *Proceedings of the Combustion Institute*, 33(1):659 – 666, 2011.

[3] J. Happold. *Geschichtete polyzyklische aromatische Kohlenwasserstoffe als Bausteine der Rußbildung*. PhD thesis, Universität Stuttgart, 2008.

[4] J. Happold, H.-H. Grotheer, and M. Aigner. Distinction of gaseous soot precursor molecules and soot precursor particles through photoionization mass spectroscopy. *Rapid Communications in Mass Spectrometry*, 21:1247–1254, 2007.

[5] J. Happold, H.-H. Grotheer, and M. Aigner. *Soot precursors consisting of stacked pericondensed PAHs*, pages 275–285. Proceedings of an International Workshop held in Villa Orlandi, Anacapri, May 13-16, 2007. Karlsruhe University Press, 2007.

[6] H. Horvath. Atmospheric light absorption a review. *Atmospheric Environment. Part A. General Topics*, 27(3):293 – 317, 1993. ISSN 0960-1686.

[7] J. Kee, K. Grcar, M. D. Smooke, and J. A. Miller. Premix: A fortran program for modelling steady laminar one-dimensional premixed flames. Technical Report 85, SANDIA National Laboratories, 1985.

[8] P. Lavvas, M. Sander, M. Kraft, and H. Imanaka. Surface chemistry and particle shape: Processes for the evolution of aerosols in titan's atmosphere. *The Astrophysical Journal*, 728(2):80, 2011.

[9] R. I. A. Patterson and M. Kraft. Models for the aggregate structure of soot particles. *Combustion and Flame*, 151:160–172, 2007.

[10] A. Raj, M. Celnik, R. Shirley, M. Sander, R. Patterson, R. West, and M. Kraft. A statistical approach to develop a detailed soot growth model using PAH characteristics. *Combustion and Flame*, 156:896–913, 2009.

[11] A. Raj, M. Sander, V. Janardhanan, and M. Kraft. A study on the coagulation of polycyclic aromatic hydrocarbon clusters to determine their collision efficiency. *Combustion and Flame*, 157(3):523–534, 2010.

[12] M. Sander. *Mathematical Modelling of Nanoparticles from the Gas-Phase*. PhD thesis, University of Cambridge, 2011.

[13] M. Sander, R. I. A. Patterson, A. Braumann, A. Raj, and M. Kraft. Developing the pah-pp soot particle model using process informatics and uncertainty propagation. *Proceedings of the Combustion Institute.*, 33:675–683, 2011.

[14] R. F. Service. Study fingers soot as a major player in global warming. *Science*, 319 (5871):1745, 2008.

[15] T. Totton, A. Misquitta, and M. Kraft. A quantitative study of the clustering of polycyclic aromatic hydrocarbons at high temperatures. Technical Report 108, c4e Preprint-Series, Cambridge, 2011.

[16] G. D. Ulrich. Special report. *Chemical & Engineering News*, 62(32):22–29, 1984.

[17] A. Violi, G. A. Voth, and A. F. Sarofim. The relative roles of acetylene and aromatic precursors during particle inception. *Proceedings of the Combustion Institute*, 30: 1343–1351, 2005.

[18] H. Wang. Formation of nascent soot and other condensed-phase materials in flames. *Proceedings of the Combustion Institute*, 33(1):41–67, 2011.

[19] H. Wang and A. Abid. *Size distribution and chemical composition of nascent soot formed in premixed ethylene flames*, pages 367–384. Proceedings of an International Workshop held in Villa Orlandi, Anacapri, May 13-16, 2007. Karlsruhe University Press, 2007.

[20] B. Zhao, Z. Yang, J. Wang, M. V. Johnston, and H. Wang. Analysis of soot nanoparticles in a laminar premixed ethylene flame by scanning mobility particle sizer. *Aerosol Science and Technology*, 37(8):611–620, 2003.

[21] B. Zhao, Z. Yang, Z. Li, M. V. Johnston, and H. Wang. Particle size distribution function of incipient soot in laminar premixed ethylene flames: effect of flame temperature. *Proceedings of the Combustion Institute*, 30(1):1441 – 1448, 2005. ISSN 1540-7489.

Citation index